

Jagged Edges: When Is Filtering Needed?

AVI C. NAIMAN

Hong Kong University of Science and Technology

Depiction of oblique edges by discrete pixels usually results in visible stair steps, often called *jaggies*. A variety of filtering approaches exists to minimize this visual artifact, but none has been applied selectively only to those edges that would otherwise appear jagged. A recent series of experiments has led to a model of the visibility of jagged edges. Here, we demonstrate how these data can be used efficiently to determine when filtering of edges is needed to eliminate the jaggies and when it is unnecessary. This work also provides a template for how the results of psychophysical experiments can be applied in computer graphics to address image-quality questions.

Categories and Subject Descriptors: I.3.3 [Computer Graphics]: Picture/Image Generation—*antialiasing*; I.4.3 [Image Processing and Computer Vision]: Enhancement—*filtering, smoothing*

General Terms: Algorithms

Additional Key Words and Phrases: Image quality, jagged edges, jaggies, visual sensitivity

1. INTRODUCTION

To display text and graphical objects on digital devices such as computer screens and printers, discrete approximations must be generated and presented. Quantization of analog representations may involve spatial, temporal, luminance, and/or chromatic channels. For presentations intended for the human eye, visual artifacts that detract from the task to be performed and from aesthetics must be identified and, if feasible, avoided or eliminated. On the other hand, if the viewer cannot distinguish between a particular displayed image and the ideal (i.e., nondiscretized) one, then there is no reason to spend further resources trying to improve on the displayed version. Because the human visual system has finite resolving ability, we are particularly interested in identifying the threshold conditions under which visual artifacts arise, and using that information in guiding engineering decisions.

This research was supported by Hong Kong's RGC DAG93/94.EG01 and CERG HKUST600/94E.

Author's address: 205 West End Avenue, #6H, New York, NY 10023-4807; email: avinaiman@acm.org.

Permission to make digital/hard copy of part or all of this work for personal or classroom use is granted without fee provided that the copies are not made or distributed for profit or commercial advantage, the copyright notice, the title of the publication, and its date appear, and notice is given that copying is by permission of the ACM, Inc. To copy otherwise, to republish, to post on servers, or to redistribute to lists, requires prior specific permission and/or a fee.

© 1998 ACM 0730-0301/98/0000-0238 \$5.00

The visual quality of computer-displayed imagery depends on numerous factors, including the display technology, the viewing environment, the visual system's (objective) capabilities and the viewer's (subjective) frame of reference (e.g., motivation, culture). Ideally, algorithms that generate images for human consumption would take all of these factors into consideration. Until comprehensive models to do so are available, we can apply what we do know about the human visual system to problems in computer graphics (see, e.g., Ferwerda et al. [1996, 1997], Greenberg et al. [1997], and Naiman and Lam [1996]) and carry out psychophysical experiments to answer specific rendering questions (whether objective or subjective); using the results to improve the image-synthesis process.¹

Here, we contribute to these goals by presenting threshold conditions under which straight edges appear jagged rather than smooth and demonstrate how to use these data efficiently to determine whether to filter a particular edge to be rendered.

1.1. Jagged Edges

Due to spatial quantization and pixel-structure artifacts, the boundaries between objects in synthesized images often appear jagged when displayed on computer screens and printers. One approach to eliminating visual artifacts in jagged edges is to increase the pixel density beyond the resolving power of the human visual system. However, given the common ability to see vernier steps as small as a few seconds of arc [Klein and Levi 1985; Westheimer 1979, 1981], it seems unlikely that technological advances will yield the required resolutions any time soon. For example, at a viewing distance of 400 mm, a 5-arc-second vernier threshold would necessitate display resolutions on the order of 100 pixels/mm, some 25 times the resolution of the high end of all but the most expensive displays currently available. Even when such increases in display resolution become more readily available, they are not the most cost-effective way to deal with "jaggies."

To attenuate the severity of these jaggies, many techniques have been developed for generating so-called "antialiased"² contours, whereby a filtering process distributes gray pixels along a boundary, giving rise to a perceived improvement in the smoothness of the contour.³ Recent contributions to the filtering literature demonstrate that this field is still quite

¹For example, Booth et al. [1987], Ferwerda and Greenberg [1988], Meyer et al. [1986], and Schwarz et al. [1987].

²Although aliasing may occur in the image-synthesis process, jaggedness is primarily due to pixel-structure artifacts that arise during reconstruction of a sampled signal by the display pixels. In fact, a completely "antialiased" image may still appear jagged, due to inexact reconstruction. Furthermore, few of the algorithms in the literature actually guarantee that the resultant sampled signal has no lower-frequency aliases. Hence, we prefer the term "filtering" rather than "antialiasing."

³See, for example, Crow [1978], Field [1984, 1986], Gupta and Sproull [1981], Pitteway and Olive [1985], and Pitteway and Watkinson [1980].

active.⁴ Because these filtering processes are inherently more computationally expensive than bilevel sampling approaches, much effort has been focused on efficiency refinements.⁵ However, despite the wealth of attention devoted to algorithm development, there are no data available on the most fundamental vision-related question relevant to such techniques: *when is filtering needed?* Due to the dearth of such data, it has not been possible to apply filtering algorithms on a conditional basis, that is, only when conditions warrant their use.

Here, we present data from a psychophysical experiment we conducted to determine the visibility⁶ of jaggedness of straight edges as a function of edge slope [Naiman and Makous 1994a, 1994b, 1995, 1996]. Although there has been some previous work on the visibility of edge raggedness and blur [Hamerly 1981; Hamerly and Springer 1981; Tyler and Mitchell 1977], ours is the first systematic account of the effects of spatial quantization on the visibility of jaggedness. These data allow us to selectively filter only those edges that would otherwise appear jagged, thereby avoiding unnecessary filtering.

To make this approach worthwhile, the process of deciding whether to filter an edge must be fast relative to the actual filtering process. To this end, we also present computationally efficient approximations to a model of the data, allowing rapid determination, for any edge slope and pixel size, of whether jaggedness will be visible and, hence, whether further computational resources should be expended to filter the edge. This preserves the important features of the psychophysical model while dealing with the practical consideration that the implementation must be fast enough to offer an advantage over a brute force, filter everything approach.

Another contribution of the work presented here is to provide a template for how the results of psychophysical experiments can be applied in computer graphics to address image-quality questions. Straight edges are just one—albeit a fundamental—component of image synthesis, and threshold detection tells us little about qualitative judgments. However, the procedures demonstrated here can be applied analogously to more complex stimuli (e.g., curves and text) as well as to questions concerning the impact of jaggedness visibility on task performance or aesthetics and the relative image-quality improvements achieved by the various filtering algorithms in use.

⁴Please see Fabris and Forrest [1997], Guenter and Tumblin [1996], Liu et al. [1996], McCool [1995], and Winner et al. [1997].

⁵For example, Barkans [1990], Winner et al. [1997], Schilling [1991], and Wu [1991].

⁶Note that visibility is an objective visual measure, characterized by averaged thresholds obtained over a number of experimental trials and for a number of representative subjects. Questions relating to ratings (e.g., which of several jagged edges appears most jagged) or preferences (e.g., which of several filtered edges is least objectionable) are subjective and, hence, more likely to depend on subject, task, and even experimental instructions.

1.2. Caveat Concerning Computational Cost of Filtering

We are assuming here that the computational cost of generating a filtered edge is substantially greater than the cost of generating an unfiltered edge. The validity of this assumption depends, of course, on the complexity of the filtering algorithm. There is a long history of developing algorithms to generate filtered versions of edges and lines at little added cost.⁷ However, all of these approaches are only approximations to idealized filtering, which is substantially more expensive (see Foley et al. [1990]). Hence, for applications in which the overhead of generating optimally filtered edges is high and the visibility of jaggedness is unacceptable, there is great value in being able to filter edges selectively.

Furthermore, filtering algorithms have, to date, made the tacit assumption that CRT display technology and the human visual system behave linearly with respect to filtered edges, that is, that the luminance generated by one pixel's setting is independent of its neighbors' settings and that the perceived subpixel position of a filtered edge bears a linear relationship to the luminance across the edge. Recent results have demonstrated that both of these assumptions are false: neighboring pixels along a CRT's scanlines exhibit strong nonlinear interactions [Naiman and Makous 1992] and the perceived subpixel position of a filtered edge depends nonlinearly on the luminance of the gray pixels [Naiman and Makous 1993a, 1993b].⁸

It is easy, therefore, to envision future rendering software that models the intricacies of the display technology, the visual system, and even the viewing environment and task. In applications that demand the highest quality edges, generating optimally filtered versions could easily take an order of magnitude longer than generating unfiltered versions. Hence, although it is beyond the scope here to quantify specific computational savings, we proceed with the assumption that determining when an edge will—and will not—appear jagged is valuable.

1.3. Caveat Concerning Pixels

The following experiment uses simulated pixels composed of 4×4 blocks of physical pixels. The blocks are square, abutting and noninteracting, and are intended to simulate a 100% fill-factor liquid-crystal display (LCD). This was chosen for the following reasons.

—Due to the introduction of spurious, easy to detect frequencies, the resultant edge profiles are the most demanding, visually speaking. Hence, the results are conservative estimates applicable to other display technologies;

⁷For example, Crow [1978], Field [1984], Gupta and Sproull [1981], Pitteway and Olive [1985], and Pitteway and Watkinson [1980].

⁸This visual nonlinearity is separate from the display's nonlinear relationship between input voltage and output luminance (commonly referred to as a display's "gamma").

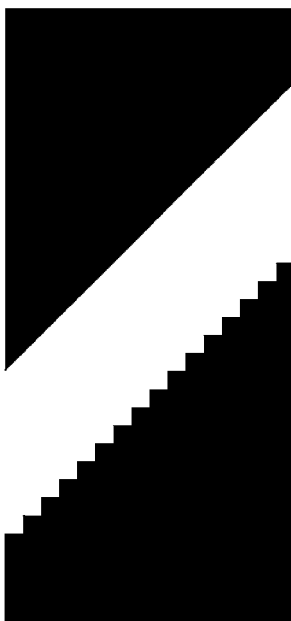


Fig. 1. A representative edge stimulus with a slope of 1.

- to explore aspects of the visual system accurately, it is crucial to know exactly what the stimuli are. Artifacts introduced by an uncharacterized display device would confound any obtained results;
- CRT displays have inherent spatial nonlinearities that distort contours and have yet to be well modeled [Naiman and Makous 1992]; and
- there is an ever-growing market of LCD and similar flat-panel displays, particularly for portable computers.

It is important, therefore, to restrict the direct application of the specific quantitative results presented here to similar display conditions. The general approaches outlined in the following, however, will be applicable to other viewing scenarios, as appropriate data become available.

2. JAGGED EDGE EXPERIMENT

To determine the human visual system's ability to detect jaggedness along a straight edge, we have embarked on a series of experiments using stimuli of the sort displayed in Figure 1. Two parallel edges are presented, differing only in polarity and size of the (simulated) pixels used to compose the edges. The subject must choose the edge that is more jagged.

2.1 Subjects

The author and three graduate students served as subjects; their ages ranged between 22 and 34. All had at least 20/20 Snellen acuity (corrected)

and otherwise normal vision, except for the anomalous trichromacy of one subject. Viewing was binocular and without head restraint.

2.2 Apparatus and Calibrations

A Mitsubishi Color Monitor (model HL7965KW-SG) was driven from a Silicon Graphics Indigo² Extreme workstation. The 1280×1024 -pixel display was 343 mm wide and 274 mm high, with pixel centers spaced every 0.268 mm on a nominally square grid. The display had a refresh rate of 60 Hz, noninterlaced, and was warmed up for 30 minutes before calibration and experimental sessions. The display's contrast adjustment was set to maximum, and the brightness adjustment was set so that a full display of maximally illuminated pixels radiated 80 cd/m^2 , as measured with a Minolta Luminance Meter (model LS-110). The black regions of the stimulus were measured at 0 cd/m^2 ; the white regions were set to 76 cd/m^2 . The size and shape of the stimuli had no effect on their luminance (cf., Naiman and Makous [1992]). Other than the stimuli, the environment was completely dark.

To distinguish the display's pixels from the blocks of pixels used to render the jagged edges, we call the former *physical pixels* and the latter *simulated pixels*. Each simulated pixel consisted of a 4×4 block of physical pixels, 1.072 mm on a side. The use of such simulated pixels rendered the effects of any nonlinear interactions between neighboring pixels insignificant [Naiman and Makous 1992].

2.3 Stimuli

For present purposes, we restrict consideration to jagged edges that are specified by integral-coordinate endpoints. The slopes of such edges are rational numbers that can be specified by a pair of integers, which we refer to as n (numerator) and d (denominator). Without loss of generality, we further restrict our discussion to jagged edges in the first octant⁹; that is, $0 < n$, $0 < d$, and $n \leq d$.

The stimulus configuration is shown in Figure 1. In each trial, simulated pixels were used to render a *jagged edge*, where each simulated pixel was turned on if the majority of its area was "covered" by the edge. We denote the straight edge drawn between the endpoints of the jagged edge as the *intended edge*, and we define the slope of the jagged edge as equal to that of the intended edge.

The set of possible slopes we considered consisted of the number of simulated pixels in the vertical direction (n), which ranged from 1 to 150, divided by the number of simulated pixels in the horizontal direction (d), which was always 150.¹⁰ To ensure a variety of jagged-edge profiles, we sampled 34 slopes from the possible 150 and presented them in either

⁹Note that, due to reflections across the horizontal and vertical axes, the actual edge stimuli appeared anywhere in the four octants flanking the horizontal axis.

¹⁰To ensure that we did not use any physical pixels near the edges of the monitor, we used a grid of 150×150 simulated pixels (i.e., 600×600 physical pixels), with allowance for the

positive or negative orientation, at random. A second *straight edge* (i.e., one in which the full resolution of the display was utilized with the same edge rendering algorithm) was rendered parallel to and offset from the jagged edge either above or below it (randomly); the orthogonal distance between the two edges was always approximately 57 mm. The size of the entire stimulus was 161 mm wide and ranged from 244 to 268 mm in height, for edge slopes ranging from near 0 to 1. Control experiments demonstrated that the edge lengths and offset distances between the edge pairs did not have a significant impact on the results.

2.4 Procedure

The subjects' task was to choose the more jagged of the two edges presented in each trial; the subjects had unlimited time to make their responses. The visual angle subtended by a simulated pixel can be varied either by changing the physical stimulus or by repositioning the subject at a different viewing distance. Owing to the constraints imposed by the physical pixels of the display and to maintain the validity of the display calibrations, we varied the visibility of the jaggedness of the edges by varying the viewing distance instead of the size of the display; the viewing distances ranged from 2 to 18.5 m. Before each test, subjects adapted to the viewing environment for at least one minute.

Subjects ran at least 250 practice trials with each of the 34 edge slopes tested. For each edge slope, five viewing distances were used over a range that yielded performance from 55 to 95% correct, as determined by preliminary tests. The order in which edge slopes were tested and the order of viewing distances for a particular edge slope were randomized for each subject. For each edge slope and viewing distance, subjects had a block of 50 trials; for each edge slope, cumulative Gaussian curves were fit by least squares to the resulting frequency-of-seeing data (with the difference between zero and the deviation of fit to each datum weighted inversely by the standard error of the fit, as estimated from binomial probability). From these curves, the *threshold viewing distance* (i.e., the distance at which performance was 75%¹¹) was estimated (see Gescheider [1985]). The reciprocal of the height of a simulated pixel (in arc minutes) at the threshold viewing distance is designated the *acuity* for that edge slope.

Note that, because one edge was composed of simulated pixels that were 4×4 times larger than the physical pixels of the other edge, when the jaggedness of the larger pixels was at threshold, the jaggedness of the smaller ones was below threshold. In fact, in almost all trials, even when the jaggedness of the edge composed of the larger pixels was above

vertical gap between the two edges. Note that there is nothing inherently special about the number 150.

¹¹Choosing 75% performance as threshold—halfway between chance and perfect performance—is conventional practice in the vision community, but is probabilistic and may not be appropriate for all applications. For example, to ensure that an edge would never appear jagged, a threshold would be called for that is closer to chance performance—50%.

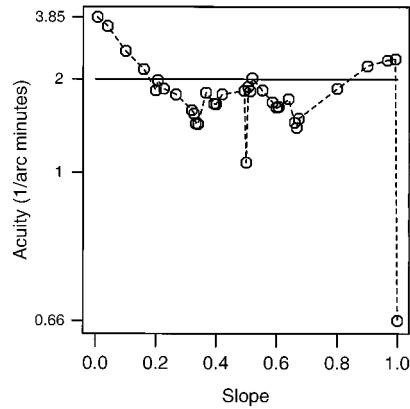


Fig. 2. Mean acuity for three subjects (on a log axis) as a function of edge slope. The horizontal line corresponds to an acuity of 2 and a pixel size of 0.5 arc minutes. The dashed line merely connects the data values and highlights the large deviations in acuity at slopes of 0.5 and 1.

threshold, the jaggedness of the edge composed of the smaller pixels was below threshold. However, at a few near viewing distances, both edges might appear jagged; hence, the instructions to the subjects were to choose the edge that appeared *more* jagged. Because the jaggedness of the edge composed of smaller pixels was almost always subthreshold—and, when it was not, the jaggedness of the other edge was clearly more visible—the experiment measured the objective visibility of edge jaggedness, and was not confounded by participants' subjective biases.

2.5 Results

The symbols in Figure 2 show the means of the acuity for three subjects as a function of edge slope. The standard errors across subjects (which, for the sake of clarity, have not been shown) are fairly uniform, at about the size of the plotted symbols, indicating a high degree of agreement across subjects. The data from the fourth subject have the same basic properties, but they were not pooled with these data because of greater acuity.

Evidently, the visibility of jaggedness depends on edge slope. In fact, a slight change in slope from 150/150 (i.e., 1) to 149/150 results in a fourfold increase in acuity (cf., the symbols closest to the lower-right and upper-right corners of Figure 2, respectively). Figure 3 shows the two stimuli used for these conditions; the reader is encouraged to view the figure from a sufficient distance to notice that the jaggedness in Figure 3(b) (slope = 150/150) can be undetectable while the jaggedness in Figure 3(a) (slope = 149/150) is clearly visible.

2.6 Practical Implications

Generally affordable soft-copy displays today have addressable resolutions between 2.5 and 4 pixels per mm. Even at the high end of this range, at a standard viewing distance of 400 mm from the display, a pixel subtends

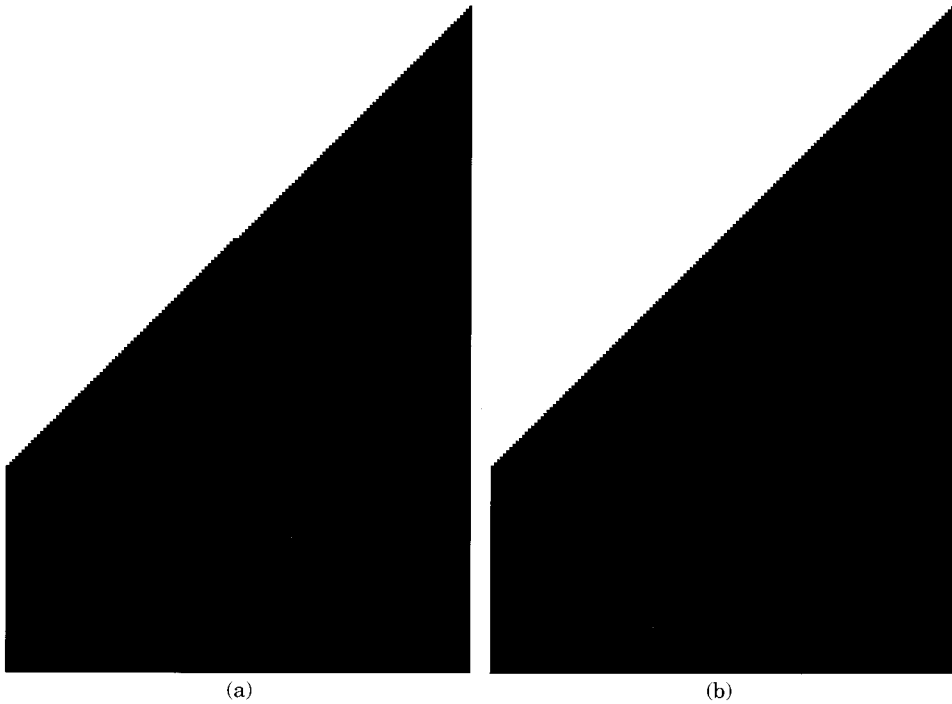


Fig. 3. The stimuli for edge slopes of (a) 149/150 and (b) 150/150 (i.e., 1). The jaggedness in (a) is four times more visible than the jaggedness in (b).

2.15 arc minutes of visual angle, corresponding to an “acuity” of 0.465. As this number is well below the bottom of the plotted region in Figure 2, jagged edges will be visible at all orientations on such devices. To make the jaggies completely disappear from black/white edges for all slopes, pixels must be no larger than that dictated by the highest acuity. For the slopes tested, the highest acuity was 3.85 (at a slope of 1/150), prescribing pixels no larger than 15.6 seconds ($60/3.85$); at a viewing distance of 400 mm, the display would require approximately 35 pixels per mm, or 17,500 pixels in each dimension of a 50 cm \times 50 cm display.

The horizontal line in Figure 2, corresponding to an acuity of 2 (and a pixel size of 0.5 arc minutes), demonstrates the visibility of jagged edges on a display with a resolution of 17 pixels per mm (when viewed from 400 mm). On such a display, high-contrast edges will appear jagged only for those slopes for which acuity is above the line; all slopes below the line will be indiscriminable from straight edges of the same orientations.

Figure 4 summarizes sensitivity to edge jaggedness in a different way: it shows how the proportion of the (e.g.) 150 edge slopes for which jaggedness would be visible depends on pixel density; the bottom scale shows density in pixels/arc min and the top one in pixels/mm at a typical CRT viewing distance of 400 mm. This figure has a number of practical implications (here we assume the 400-mm viewing distance).

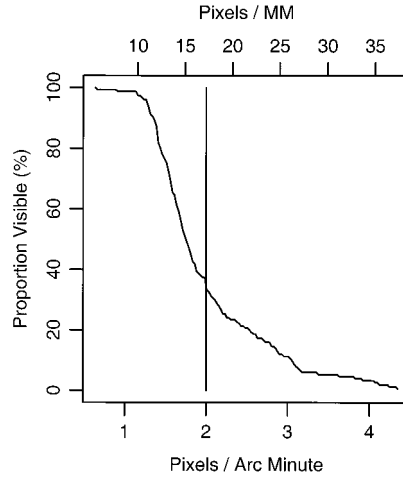


Fig. 4. The dependence of the proportion of edge slopes for which jaggedness would be visible on pixel density; the bottom scale shows density in pixels/arc min and the top scale shows density in pixels/mm at the standard CRT viewing distance of 400 mm. The vertical line corresponds to a pixel size of 0.5 arc min (cf. the horizontal line in Figure 2), for which about 35% of the slopes will appear jagged.

- Even if a display contains as many as 6 pixels/mm, edges on such a display would be visibly jagged at all slopes except those that are exactly horizontal or vertical.
- At a pixel density of about 2 pixels/arc min, or 17 pixels/mm, the proportion of edges that are visibly jagged decreases to about 35%. Reference to Figure 2 shows that the visibly jagged edges have slopes below about 0.2 and above about 0.8 (not including 1.0).
- To ensure that no edge appears jagged, a pixel density of about 35 pixels/mm is required.

Reference to Figure 2 shows that, to minimize the prevalence of visibly jagged edges, one can restrict edge slopes to multiples of 22.5° . Even where such restrictions are impractical, one can take advantage of the fact that changes in the slope of a contour can be made without being noticed, and even noticeable changes may nevertheless be tolerable. How much of a change in slope is required in order to be noticed depends on many variables. Under the best of conditions, changes of 20 arc minutes cannot be detected, and, if the line is oblique, a change of one degree cannot be detected; under less than optimal conditions, much larger changes—up to four degrees or more—can be made without being noticed [Heeley et al. 1997; Li and Westheimer 1997]. This means, for example, that the slope of the most visibly jagged edge on the right side of Figure 2 can be changed to the slope that has the least visible jaggedness, 45° , without a noticeable change of slope, and, possibly, the slopes of the two other most visibly jagged edges could likewise be changed to 45° without any noticeable (or, at least, intolerable) change of slope.

3. DETERMINING WHICH EDGES NEED FILTERING

In this section, our goal is to determine whether the jaggedness of an edge rendered from (x_1, y_1) to (x_2, y_2) will be visible. If the edge will appear jagged, we want to filter the edge; however, if the unfiltered edge will not appear jagged, we want to avoid unnecessary filtering, a potentially expensive process, particularly if the filtering process takes into consideration display [Naiman and Makous 1992] and visual system [Naiman and Makous 1993a, 1993b] nonlinearities. Of course, the process to determine the visibility of the jaggedness must be quick enough to warrant the overhead incurred by this test for rendering each edge.

3.1. Number of Unique Edges in a Display

Before we outline the process for determining the visibility of a jagged edge, let us examine how many unique edges there are in a raster display, with respect to unique visual acuities of edge jaggedness.

In a raster display with n rows and n columns, one can render an edge between $n^2 \times (n^2 - 1)$ pairs of pixels. Although these edges are all unique in their endpoint specifications, many of them are identical to each other with regard to their effect on the visual system. For example, the edge from (x_1, y_1) to (x_2, y_2) has the same effect on the visual system as the edge from (x_2, y_2) to (x_1, y_1) . Similarly, the edge from (x_1, y_1) to (x_2, y_2) has the same effect on the visual system as the edge from $(x_1 + \Delta x, y_1)$ to $(x_2 + \Delta x, y_2)$.

By capitalizing on the symmetries of reflection about the horizontal, vertical, and diagonal axes, we can, without loss of generality, restrict consideration to those edges with slopes in the range $[0, 1]$. On its own, this constraint leads only to an eightfold reduction in the number of unique edges. However, we can further restrict consideration to those edges that are not translations of any other edge. Taken together, these constraints limit our consideration only to those edges from $(x_1 = 0, y_1 = 0)$ to $(0 < x_2 < n, 0 \leq y_2 \leq x_2)$; there are only $\sum_{i=2}^n i = (n(n + 1))/2$ such unique edges.

There is one further constraint we can place on edge uniqueness. Consider the edge from $(0, 0)$ to (x, y) (x and y both even) and the edge with the identical slope, but half the length, that is, from $(0, 0)$ to $(x/2, y/2)$. These edges will have nearly identical effects on the visual system. In fact, except for very short edges, all edges of the same slope will have similar visibility, with greatest visual sensitivity for the longest one. Hence, we can consider only edges with unique slopes; to be conservative, all edges with the same slope but different lengths should be assumed to have the visibility of the longest of these edges.

Determining the number of unique slopes of edges rooted at $(0, 0)$ in the first octant is identical to determining the number of relatively prime x - y pairs in the first octant; asymptotically, this is $(6/\pi^2) + O(\log n/n)$ [Graham et al. 1989]; for large enough n , this value is approximately 60%. Although this final constraint does not reduce the computational complex-

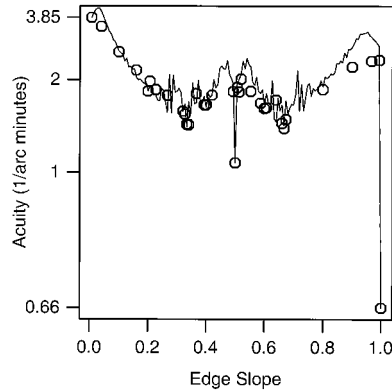


Fig. 5. The data from Figure 2 overlaid with predictions of an acuity model (solid line); calculations were made at each of the 150 possible edge slopes and line segments were drawn to connect these values.

ity from $O(n^2)$, the 40% savings could conceivably be worthwhile. For our purposes, on a $1,024 \times 1,024$ -pixel display, there are $(0.6 \times 1,024(1,024 + 1))/2 \approx 315,000$ unique edges.

Now that we've determined the unique slopes of interest, we are ready to determine, for each of the corresponding edges, whether the jaggedness will be visible.

3.2. Visibility of Edge Jaggedness in a Display

To determine whether an arbitrarily oriented edge needs filtering, we need the ability to predict jaggedness acuity for untested slopes. In Figure 5, the datapoints obtained in the experiment have been overlaid with the predictions of just such an acuity model that we have developed to fit this data set, based on employing the one-dimensional Fourier transform of the edge profiles and a function describing sensitivity to sinusoidal modulation of edges [Hamerly and Springer 1981]. Specific details of the model are beyond the scope and intent of this article; a summary of the model is provided in the Appendix.

Given the slope of an edge, this acuity model can be used to compute the visual acuity to jaggedness, which is the inverse of threshold pixel size. If an individual pixel in a particular display subtends, at a specific viewing distance, an angle smaller than the threshold pixel size, then the jaggedness will be imperceptible. Conversely, for any given acuity, the viewing distance can be increased until the angle subtended by a pixel is below the corresponding threshold.

Figure 6 shows the relative acuities for all the edges in the first octant of a 64×64 -pixel display (a 64×64 display is used rather than 150×150 to ensure the visibility of individual elements of the matrix). Each (x, y) pixel in the figure that is below or on the main diagonal has a grayscale value proportional to the jaggedness acuity of an edge from $(0, 0)$ to (x, y) , with

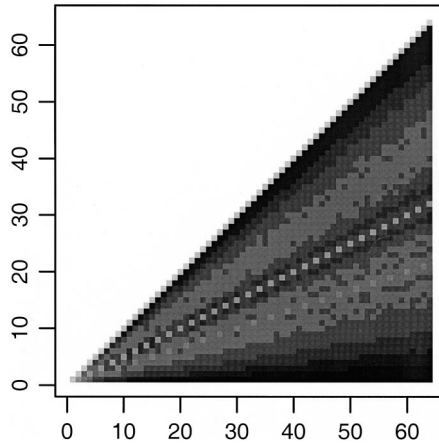


Fig. 6. The relative acuities for all unique edges in a 64×64 -pixel display, with darker pixels corresponding to higher acuities.

darker grays corresponding to higher acuity (i.e., the need for smaller pixels).

To understand this figure, examine the far right column of gray values. The bottom-most gray value, at $(63, 1)$, corresponds to an edge from $(0, 0)$ to $(63, 1)$, with a slope of $1/63$; the dark gray indicates the relatively high acuity to jaggedness at this slope. The top-most gray value, at $(63, 63)$, corresponds to an edge from $(0, 0)$ to $(63, 63)$, with a slope of 1; the light gray indicates the relatively low acuity to jaggedness at this slope. In fact, all of the locations along the main diagonal have a slope of 1 and correspondingly low acuity. In each column, the location just below the main diagonal, $(x, x - 1)$, corresponds to an edge with a slope of $(x - 1)/x$, which always has a relatively high acuity. Note the series of light gray pixels in alternating columns ascending in the middle of the triangle; these pixels correspond to a slope of 0.5, which has relatively low acuity (cf. Figure 2).

If computing the model's prediction for a given edge was a quick operation, we could dynamically generate these acuity data as needed. However, the computations are quite complex; therefore, it is necessary to precompute this grayscale array of acuities at the spatial resolution of the designated display. Then, just before rendering an edge, the corresponding slope vector can be used to look up the acuity in the array, determining if the display's pixel size is larger than the indicated threshold pixel size and, therefore, whether filtering of the edge is needed.

Now, reconsider the horizontal line in Figure 2, corresponding to a display with a pixel size of 0.5 arc minutes of visual angle. The jaggedness of all edges with acuities above that line are visible, and those below the line are not. Because typical computer usage involves a fixed viewing distance from the display, we can, analogously, prethreshold the grayscale acuity array from Figure 6, generating a Boolean (i.e., 1-bit) version of the array, which can be more efficient to store and use in comparison tests.

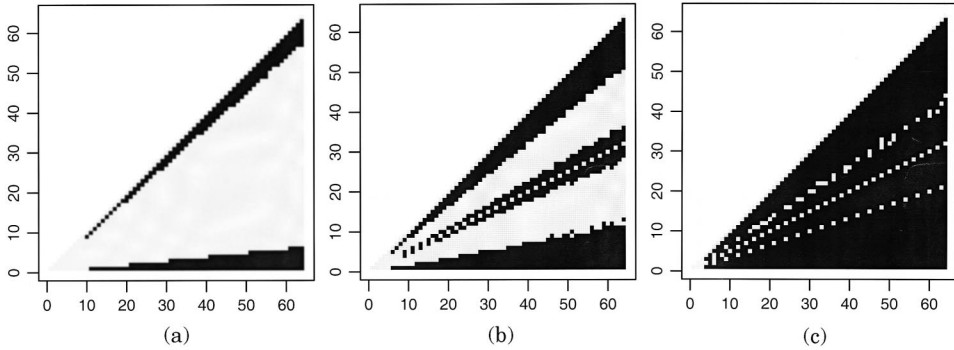


Fig. 7. Boolean acuity arrays computed by thresholding the grayscale array in Figure 6 at pixel sizes: (a) 0.4 arc min.; (b) 0.6 arc min.; and (c) 0.8 arc min.; black pixels correspond to edges above threshold.

Figure 7 shows three such Boolean arrays, prethresholded for pixel sizes ranging from 0.4 to 0.8 minutes. Changing the viewing distance requires computing a new (threshold) version of the array, but this need be done only once per viewing distance.

3.3. First-Order Approximations to Jaggedness Visibility

The approach described up to now has required the precomputation of the grayscale acuity array, by applying the acuity model to each edge. The advantage of this approach is that acuities corresponding to all unique edges are computed and refinements to the model, such as incorporating the effects of pixel shapes and interactions, can be applied in a straightforward manner. However, if a first-order approximation to the acuity model is satisfactory, then regression fits to the data (Figure 8) can be used to obviate the need for the grayscale and Boolean acuity arrays altogether.

In this case, the following approaches can be taken: (1) for any specific edge slope, the intersection between the edge slope (along the figure's x -axis) and the relevant regression line segment is computed, taking care to handle edge slopes of 0.5 and 1 as special cases; or (2) a lookup table of acuities is precomputed from these intersections, at the resolution of the linear size of the display (e.g., 1,024); acuities corresponding to intermediate edge slopes are computed by interpolation.

The regression fits in Figure 8 can be approximated with the parameters in Table I. Recall that the plot in Figure 8 is log-linear. As an asymptote of 0.614 was used in the plots, the actual acuity values are obtained from $10^{es \times rfs + rfi} + 0.614$, where es is the slope of the edge, rfs is the slope of the regression fit, and rfi is the intercept of the regression fit. Table II lists the acuities obtained by these approximations, for all edge slopes in the right-hand column of Figure 6. All other edge slopes from Figure 6 can be obtained by interpolating the values in the table. Fixed-point representations of the edge slopes and acuities can be used to speed up the comparisons needed at runtime.

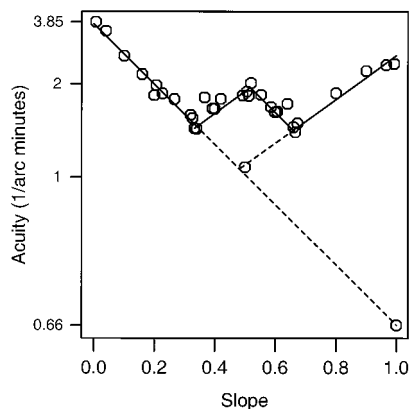


Fig. 8. The data from Figure 2 overlaid with regression fits (solid lines). The points corresponding to slopes of 0.5 and 1 lie on the dashed extensions of the exterior diagonal lines.

Table I. Regression Fits

Edge Slope Range	Regression Fit Intercept	Regression Fit Slope
[0, 1/3]	0.52	-1.82
[1/3, 0.5)	-0.53	1.22
0.5	0.52	-1.82
(0.5, 2/3]	0.87	-1.52
[2/3, 1)	-0.98	1.25
1.0	0.52	-1.82

In summary, the process of using the first-order approximations to determine if an edge from (x_1, y_1) to (x_2, y_2) on a (e.g.) $1,024 \times 1,024$ -pixel display would appear jagged to a viewer and, hence, need filtering, consists of the following steps.

Precomputation:

Choose a *Viewing Distance*

Determine *Pixel Size* in Arc Minutes at *Viewing Distance*

Generate 1,024-Element *Acuity* Lookup Table Using Formulas from Table I

Generate *Reciprocals* of *Acuity*

Generate *Visibility_Thresholds* by Thresholding *Reciprocals* with *Pixel Size*.

For an Edge from (x_1, y_1) to (x_2, y_2) :

$slope = |y_2 - y_1| / |x_2 - x_1|$

If $slope > 1$ **Then** $slope = 1/slope$

$slope = slope \times 1,024$

$visible = Visibility_Thresholds[Round(slope)]$

If $visible$ is TRUE **Then** Filter Edge **Else** Render Bilevel Edge.

In this nonoptimized formulation the runtime overhead for this process consists of three or four assignments, two tests, one table lookup, two integer subtractions, two absolute values, one rounding operation, one multiplication, and one or two divisions. Hence, the overhead—particularly

Table II. Approximated Acuities

Edge Slope	Acuity (minutes)	Edge Slope	Acuity (minutes)	Edge Slope	Acuity (minutes)	Edge Slope	Acuity (minutes)
1/64	3.73	17/64	1.71	33/64	1.82	49/64	1.56
2/64	3.53	18/64	1.64	34/64	1.76	50/64	1.61
3/64	3.35	19/64	1.58	35/64	1.7	51/64	1.65
4/64	3.18	20/64	1.51	36/64	1.64	52/64	1.7
5/64	3.01	21/64	1.46	37/64	1.59	53/64	1.75
6/64	2.86	22/64	1.39	38/64	1.54	54/64	1.8
7/64	2.72	23/64	1.43	39/64	1.49	55/64	1.86
8/64	2.59	24/64	1.46	40/64	1.44	56/64	1.91
9/64	2.46	25/64	1.5	41/64	1.4	57/64	1.97
10/64	2.35	26/64	1.54	42/64	1.35	58/64	2.03
11/64	2.24	27/64	1.58	43/64	1.34	59/64	2.1
12/64	2.13	28/64	1.62	44/64	1.37	60/64	2.17
13/64	2.04	29/64	1.67	45/64	1.41	61/64	2.24
14/64	1.95	30/64	1.72	46/64	1.44	62/64	2.31
15/64	1.86	31/64	1.77	47/64	1.48	63/64	2.39
16/64	1.78	32/64	1.03	48/64	1.52	64/64	0.66

in an optimized version—is a substantial reduction in computation as compared to the complete filtering process. Note, however, that these approximations depend on the edge-drawing algorithm generating the standard edge profile corresponding to turning on any (and only those) pixels that are at least half-covered by the edge.

4. CONCLUSIONS

It is well known that the visual system can detect jagged edges. Until now, an all-or-nothing decision had to be made as to whether to filter the edges in an image. We have shown how to apply quantitative data from a visual acuity experiment to allow slope-dependent determination of which edges need filtering. Because the acuity data can be precomputed and stored in a lookup table, the test for whether to filter an edge adds little overhead to the edge-rendering process and provides the potential for great computational savings.

The simulated pixels we used are the most demanding vis-a-vis edge jaggedness: square, nonoverlapping pixels with sharp luminance profiles. Hence, the acuity data presented here are conservative, particularly with respect to CRT-based display systems, which filter out much of the high-frequency spectra in edges. We would expect to find lower sensitivity to jaggedness when using a CRT's full resolution, simply because the displayed edges are physically smoother. However, the specific degree of edge smoothing depends on a variety of factors, including the video signals, display type, control settings, and equipment age. Future models of the

distortions imposed by various display technologies may allow for device-dependent acuity models. In the meantime, the results summarized here, which represent the limits of the visual system, can be used as conservative estimates of the visibility of edge jaggedness.

The acuity data presented here are threshold measurements that tell us the boundary conditions for when filtering of an edge can have a visual impact. These results, however, strictly apply only to static, high-contrast, black/white edges in isolation; for now, though, they are also our best estimates of the visibility of jaggedness of low-contrast, colored, touching, and/or moving edges. Note that it is still an open question as to how to *best* filter edges: threshold results tell us only *when* filtering is needed. This has relevance even to the unfiltered edge, because an image in which some edges are left unfiltered and others are filtered suboptimally may be disconcerting. Similar visual artifacts might exist for a rotating edge that is left unfiltered at certain orientations and is (perhaps suboptimally) filtered at other orientations.

Psychophysical experiments like the one presented here can help us answer many questions related to image quality. A natural extension of this work is to apply the approaches outlined here to collect acuity data on sensitivity to jaggedness of lines, curves, and higher-level graphic components, such as text, as well as to determine the perceived subpixel position of jagged edges that have been filtered. We believe that the systematic approach of using human vision models to optimize rendering will be the foundation of future graphics algorithms, whether low-level and objective, as demonstrated here, or high-level and subjective, such as rating the aesthetics of various ray tracing algorithms (see Greenberg et al. [1997]). This presentation augments traditional approaches in computer graphics by familiarizing researchers with why psychophysical experiments are designed, how they are executed practically, and how the results can be applied to the image-synthesis process.

APPENDIX. VISION MODEL

The fact that luminance is binary in this experiment greatly simplifies the problem of describing the jagged edge, for the shape of the boundary defining the edge can be decomposed by a *one-dimensional* Fourier analysis; that is, the step displacement associated with a vernier acuity target can be regarded as the sum of a set of sinusoidally modulated functions that have a $1/f$ amplitude spectrum. To relate these Fourier components to sensitivity, one requires a function describing sensitivity to the different basis functions comprising the edge.

Hamerly and Springer [1981] measured sensitivity to edges with boundaries that were modulated sinusoidally, determining threshold amplitude as a function of the frequency of the modulation. They found a bandpass threshold function with a minimum at around eight cycles per degree (cpd) of visual angle. They also tested sensitivity to boundaries composed of the sum of pairs of sine waves with frequency ratios of 3:1 and various relative

phases. Their results provide evidence that detection of such patterns is performed by a set of independent channels that are selectively sensitive to restricted frequency bands.

We find that the data of Hamerly and Springer are well described by a Gaussian function:

$$T(f) = a \left(1.07 - \exp\left(-\frac{1}{2}\left(\frac{f-8}{20}\right)^2\right) \right), \quad (1)$$

where f is spatial frequency in cpd and a is a free parameter that equals 0.4 for Hamerly and Springer's data. The curve has a minimum ($a \cdot 0.07$) at 8 cpd, and so it has what is often called a *low-frequency cut*. To scale the magnitude of this cut, we introduce a free parameter c :

$$T'(f) = c \cdot T(f) + (1 - c)(a \cdot 0.07), \quad c = 1, \quad \text{where } f > 8. \quad (2)$$

The shape and height of this curve depend on many variables specific to the situation in which it is tested. The aspects of this curve that are likely to be most variable are its height (a in Eq. 2) and the magnitude of the low-frequency cut (c). Accordingly, we have used the shape of this function in our modeling but left parameters controlling these two aspects of the curve free; we call Eq. 2 a *generalized Hamerly–Springer threshold function*. We find that our data are best described if we assume that the rise of thresholds at frequencies below the minimum of the function (i.e., 8 cpd) is one-fifth as great as it was in Hamerly and Springer's experiment (i.e., $c = 0.2$). For the mean data of the three subjects reported here, $a = 1.04$, whereas for the fourth subject, $a = 0.66$. This discrepancy may be explained by the fact that the three subjects pooled together were not highly practiced and vernier acuity is known to be highly sensitive to practice. The value required for Hamerly and Springer's data, $a = 0.4$, falls outside the range for our subjects, but the difference is not excessive in view of the differences among our own subjects and the differences between experimental conditions.

Although Hamerly and Springer have shown that Fourier components at frequencies differing by a factor of three are detected independently, components that are closer in frequency can be expected to combine their effects on visibility. To describe such combined effects, we have assumed that the effect of any given Fourier component is augmented in proportion to the amplitudes of the neighboring components, each weighted according to a Gaussian function of its distance on a logarithmic scale. Specifically, the excitation E_i , associated with the Fourier component at frequency f_i , is the sum of the weighted contributions of all Fourier components at frequencies f_j :

$$E_i(f_i) = \sum_{j=1}^{\infty} A_j \exp\left(-\frac{(\log_{10} f_j - \log_{10} f_i)^2}{2s^2}\right), \quad (3)$$

where A_j is the amplitude of the Fourier component at frequency f_j . The spread of the Gaussian, s , is a free parameter in our model that had the value of $0.05 \log_{10}$ units.

To determine the visibility of the jaggedness of an edge of a particular slope at a particular distance, we first compute the one-dimensional Fourier transform of the edge boundary at that distance. If any of the Fourier components is at or above the threshold defined by the generalized Hamerly–Springer function, we consider the jagged edge to be discriminable from a straight edge. To determine the jaggedness detection threshold for a jagged edge of a particular slope, we choose the farthest distance that places at least one of the Fourier components at threshold.

This procedure was carried out to compute the model's predicted acuities for a variety of parameter settings: we varied each parameter independently, computed the squared differences between the data and the model, and plotted the results with the data. The line in Figure 5 passes through the predictions obtained for each of the 150 possible edge slopes, where $a = 1.04$, $c = 0.2$, and $s = 0.05$. Note that the model follows the complexities of the data, including the large discontinuities at slopes of 0.5 and 1.0.

ACKNOWLEDGMENTS

I thank Ada Yuen, Ivan Wong, and Desamanya Peramunetilleke for serving as subjects in these experiments and Walter Makous, Alain Fournier, Michael S. Landy, Denis G. Pelli, Annette Werner, and the anonymous reviewers for helpful comments. I am grateful to the Department of Psychology at New York University for providing facilities with which to prepare this manuscript.

REFERENCES

- BARKANS, A. C. 1990. High speed high quality antialiased vector generation. *Comput. Graph.* 24, 4 (Aug.), 319–326; *Proceedings SIGGRAPH '90* (Dallas, TX, Aug. 6–10). ACM, New York, NY.
- BOOTH, K. S., BRYDEN, M. P., COWAN, W. B., MORGAN, M. F., AND PLANTE, B. L. 1987. On the parameters of human visual performance: An investigation of the benefits of antialiasing. *IEEE Comput. Graph. Appl.* 7, 9 (Sept.), 34–41.
- CROW, F. C. 1978. The use of grayscale for improved raster display of vectors and characters. *Comput. Graph.* 12, 3 (Aug.), 1–6; *Proceedings SIGGRAPH '78* (Atlanta, GA, Aug. 23–25). ACM, New York, NY.
- FABRIS, A. E., AND FORREST, A. R. 1997. Antialiasing of curves by discrete pre-filtering. In *SIGGRAPH 97 Conference Proceedings* (Los Angeles, CA, Aug. 3–8), ACM, New York, NY, 317–326.
- FERWERDA, J. A. AND GREENBERG, D. P. 1988. A psychophysical approach to assessing the quality of antialiased images. *IEEE Comput. Graph. Appl.* 8, 5 (Sept.), 85–95.
- FERWERDA, J. A., PATTANAIK, S. N., SHIRLEY, P., AND GREENBERG, D. P. 1996. A model of visual adaptation for realistic image synthesis. In *SIGGRAPH 96 Conference Proceedings* (New Orleans, LA, Aug. 4–9), ACM, New York, NY, 249–258.
- FERWERDA, J. A., PATTANAIK, S. N., SHIRLEY, P., AND GREENBERG, D. P. 1997. A model of visual masking for computer graphics. In *SIGGRAPH 97 Conference Proceedings* (Los Angeles, CA, Aug. 3–8), ACM, New York, NY, 143–152.

- FIELD, D. 1984. Two algorithms for drawing anti-aliased lines. In *Proceedings of Graphics Interface 1984* (Ottawa, Ont., May 28–June 1), 87–95.
- FIELD, D. 1986. Algorithms for drawing anti-aliased circles and ellipses. *Comput. Vis. Graph. Image Process.* 33, 1–15.
- FOLEY, J. D., VAN DAM, A., FEINER, S. K., AND HUGHES, J. F. 1990. *Computer Graphics: Principles and Practice*. Addison-Wesley, Menlo Park, CA.
- GESCHIEDER, G. A. 1985. *Psychophysics: Method, Theory and Application*, Second Edition. Lawrence Erlbaum Associates, Hillsdale, NJ.
- GRAHAM, R. L., KNUTH, D. E., AND PATASHNIK, O. 1989. *Concrete Mathematics: A Foundation for Computer Science*. Addison-Wesley, Reading, MA.
- GREENBERG, D. P., ARVO, J., LAFORTUNE, E., TORRANCE, K. E., FERWERDA, J. A., WALTER, B., TRUMBORE, B., SHIRLEY, P., PATTANAIK, S. N., AND FOO, S.-C. 1997. A framework for realistic image synthesis. In *SIGGRAPH 97 Conference Proceedings* (Los Angeles, CA, Aug. 3–8), ACM, New York, NY, 477–494.
- GUENTER, B. AND TUMBLIN, J. 1996. Quadrature prefiltering for high quality antialiasing. *ACM Trans. Graph.* 15, 4 (Oct.), 332–353.
- GUPTA, S. AND SPROULL, R. F. 1981. Filtering edges for gray-scale displays. *Comput. Graph.* 15, 3 (Aug.), 1–5; *Proceedings SIGGRAPH '81* (Dallas, TX, July). ACM, New York, NY.
- HAMERLY, J. R. 1981. An analysis of edge raggedness and blur. *J. Appl. Photograph. Eng.* 7, 6 (Dec.), 148–151.
- HAMERLY, J. R. AND SPRINGER, R. M. 1981. Raggedness of edges. *J. Opt. Soc. Am.* 71, 3 (March), 285–288.
- HEELEY, D. W., BUCHANAN-SMITH, H. M., CROMWELL, J. A., AND WRIGHT, J. S. 1997. The oblique effect in orientation acuity. *Vis. Res.* 37, 2 (Jan.), 235–242.
- KLEIN, S. A. AND LEVI, D. M. 1985. Hyperacuity thresholds of 1 second: Theoretical predictions and empirical validation. *J. Opt. Soc. Am. A* 2, 7 (July), 1170–1190.
- LI, W. AND WESTHEIMER, G. 1997. Human discrimination of the implicit orientation of simple symmetrical patterns. *Vis. Res.* 37, 5 (March), 565–572.
- LIU, N., JIN, H., AND ROCKWOOD, A. P. 1996. Antialiasing by Gaussian integration. *IEEE Comput. Graph. Appl.* 16, 3 (May), 58–63.
- MCCOOL, M. D. 1995. Analytic antialiasing with prism splines. In *SIGGRAPH 95 Conference Proceedings* (Los Angeles, CA, Aug. 6–11), ACM, New York, NY, 429–436.
- MEYER, G. W., RUSHMEIER, H. E., COHEN, M. F., GREENBERG, D. P., AND TORRANCE, K. E. 1986. An experimental evaluation of computer graphics imagery. *ACM Trans. Graph.* 5, 1 (Jan.), 30–50.
- NAIMAN, A. C. AND LAM, D. T. W. 1996. Error diffusion: Wavefront traversal and contrast considerations. In *Proceedings of Graphics Interface 1996* (Toronto, Ont., May 21–24), 78–86.
- NAIMAN, A. C. AND MAKOUS, W. 1992. Spatial non-linearities of grayscale CRT pixels. In *SPIE Proceedings: Human Vision, Visual Processing and Digital Display III* (San Jose, CA, June 14–16), Vol. 1666, 41–56.
- NAIMAN, A. C. AND MAKOUS, W. 1993a. Undetected gray strips displace perceived edges nonlinearly. *J. Opt. Soc. Am. A* 10, 5 (May), 794–803.
- NAIMAN, A. C. AND MAKOUS, W. 1993b. Information transmission for sub-pixel edge positioning. *J. Soc. Inf. Disp.* 1, 4 (Dec.), 437–447.
- NAIMAN, A. C. AND MAKOUS, W. 1994a. Jagged edges and their visibility. *Soc. Inf. Disp. 94 Digest* 25, (June), 205–208.
- NAIMAN, A. C. AND MAKOUS, W. 1994b. Computing the jaggedness of edges. In *Proceedings of the Fourth International Conference on Computer-Aided Drafting, Design and Manufacturing Technology: Pacific Graphics '94/CADDM '94* (Beijing, Aug. 26–29), 41–45.
- NAIMAN, A. C. AND MAKOUS, W. 1995. The visibility of higher-level jags. *Soc. Inf. Disp. 95 Digest* 26 (May), 113–116.
- NAIMAN, A. C. AND MAKOUS, W. 1996. Vernier acuity modeled by one-dimensional Fourier analysis. *Invest. Ophthalm. Vis. Sci.* 37, 3 (Feb.), S734.

- PITTEWAY, M. L. V. AND OLIVE, P. M. 1985. Filtering edges by pixel integration. *Comput. Graph. Forum* 4, 2 (June), 111–116.
- PITTEWAY, M. L. V. AND WATKINSON, D. J. 1980. Bresenham's algorithm with grey scale. *Commun. ACM* 23, 11 (Nov.), 625–626.
- SCHILLING, A. 1991. A new simple and efficient antialiasing with subpixel masks. *Comput. Graph.* 25, 4 (July), 133–141; *Proceedings SIGGRAPH '91* (Las Vegas, NV, July 28–Aug. 2), ACM, New York, NY.
- SCHWARZ, M. W., COWAN, W. B., AND BEATTY, J. C. 1987. An experimental comparison of RGB, YIQ, LAB, HSV and opponent color models. *ACM Trans. Graph.* 6, 2 (April), 123–158.
- TYLER, C. W. AND MITCHELL, D. E. 1977. Orientation differences for perception of sinusoidal line stimuli. *Vis. Res.* 17, 83–88.
- WESTHEIMER, G. 1979. Proctor lecture: The spatial sense of the eye. *Invest. Ophthalm. Vis. Sci.* 18, 893–912.
- WESTHEIMER, G. 1981. Visual hyperacuity. In *Progress in Sensory Physiology* 1. H. Autrum, D. Ottoson, E. R. Perl, and R. F. Schmidt, Eds., Springer-Verlag, New York, 1–30.
- WINNER, S., KELLEY, M., PEASE, B., RIVARD, B., AND YEN, A. 1997. Hardware-accelerated rendering of anti-aliasing using a modified A-buffer algorithm. In *SIGGRAPH 97 Conference Proceedings* (Los Angeles, CA, Aug. 3–8), ACM, New York, NY, 307–316.
- WU, X. 1991. An efficient antialiasing technique. *Comput. Graph.* 25, 4 (July), 143–152; *Proceedings SIGGRAPH '91* (Las Vegas, NV, July 28–Aug. 2), ACM, New York, NY.

Received July 1997; revised December 1997; accepted April 1998